DOI: 10.1002/ejic.200901045

Towards Fluoride Sensing with Positively Charged Lanthanide Complexes

Raphaël Tripier,*[a] Carlos Platas-Iglesias,[b] Anne Boos,[c] Jean-François Morfin,[a] and Loïc Charbonnière*[c]

Dedicated to Professor Jean-Claude Bünzli on the occasion of his 65th birthday

Keywords: Lanthanides / Macrocyclic ligands / Luminescence / Anions / Sensors

Herein we report a series of $[Ln\mathbf{L}(H_2O)]Cl_3$ complexes, in which **L** is a 1,4,7,10-tetrazacyclododecane framework (cyclen) functionalized with 2-methylpyridyl pendants on the nitrogen atoms at the 1- and 7-positions and with *N*-[2-(2-hydroxyethoxy)ethyl]acetamide groups on those at the 4- and 10-positions, and Ln stands for Eu, La, and Tb. The complexes were isolated and characterized by elemental analysis, mass spectrometry, infrared spectroscopy, and ^{1}H NMR spectroscopy for the La and Eu complexes. ^{1}H NMR spectroscopy indicates that the complexes display a major twisted square antiprismatic (TSAP) geometry in solution, which was confirmed by using DFT calculations. ^{1}H and ^{13}C variable-temperature NMR spectroscopic experiments on the La complex provided an activation free energy of $\Delta G^{\neq} = (58 \pm 3)$ kJ mol^{-1} for the enantiomerization process of the TSAP isomer, which requires both the inversion of the five-membered chelate rings formed upon coordination of the cyclen moiety and the rotation of the pendant arms. The photophysical properties of the complexes were studied by means of absorption, steady-state, and time-resolved luminescence spectroscopy. Upon ligand excitation, the Eu and Tb complexes displayed the typical lanthanide-centered emission spectra with weak emission efficiencies (Φ_{ov} = 0.11 and 0.68 %, respectively, for Eu and Tb in H_2O). Luminescence lifetime measurements in water and heavy water allowed the determination of the hydration number of the complexes; these were (1.0 ± 0.2) for Eu and Tb. Spectrophotometric titrations of the $[Ln\mathbf{L}(H_2O)]Cl_3$ complexes (Ln = Eu and Tb) with F^-, Cl^-, and Br^- anions (in buffered water solutions, 0.01 M tris(hydroxymethyl)aminomethane (TRIS)/$HClO_4$, pH = 7.0) showed the complexes to interact selectively with fluoride anions, whereas no interactions were observed with Cl^- and Br^-. The interaction with F^- was monitored by luminescence spectroscopy with $[Eu\mathbf{L}(H_2O)]$, which evidenced dramatic changes in the shape of the luminescence spectra, and an association constant of (2.86 ± 0.06) log units was determined. In the case of the Eu complex, time-resolved and high-resolution emission spectroscopy showed that the interaction resulted in the displacement of the coordinated water molecule, which led to an increase of the overall luminescence quantum yield, with almost no impact on the ligand-to-metal sensitization efficiency. Investigation of the Eu and La complexes by potentiometry (0.1 M NaCl) allowed the determination of the protonation constants of the complexes as well as the association constants with fluoride anions. DFT calculations on the fluoride adduct of the Eu complex confirmed the higher stability of the TSAP isomer and evidenced large structural changes upon F^- binding, in agreement with spectrophotometric observations in solution.

Introduction

Bonds formed between lanthanide(III) cations and their ligands are generally assumed to be purely electrostatic in nature, even if a small degree of covalency has been proposed.[1] The electronegativity of the donor atom(s) and the steric factors of the ligand then govern the strength of such bonds, and one can expect that the interaction between lanthanide complexes and fluoride will be rather strong, fluorine being the most electronegative element of the periodic table according to Pauling's classification. Such a strong binding should then be considered for various applications related to either lanthanide complexes or fluoride anions. As an example, the addition of large amounts of KF is known to improve the luminescence of europium cryptates[2] within the framework of lanthanide-based time-resolved fluoro-immunoassays.[3] These macrobicyclic complexes do not fully saturate the first coordination sphere of the Ln^{III} cations, thus leaving space for the coordination of

[a] Université de Bretagne Occidentale,
UMR-CNRS 6521/IFR148 ScInBioS, UFR des Sciences et Techniques,
6 avenue Victor le Gorgeu, C.S. 93837, 29238 Brest Cedex 3, France
[b] Departamento de Química Fundamental, Universidade da Coruña,
Alejandro de la Sota 1, 15008 A Coruña, Spain
[c] Laboratoire d'Ingénierie Moléculaire Analytique,
UMR 7178 CNRS, IPHC, ECPM,
25 rue Becquerel, 67087 Strasbourg Cedex, France
E-mail: l.charbonn@chimie.u-strasbg.fr

Supporting information for this article is available on the WWW under http://dx.doi.org/10.1002/ejic.200901045.

 © 2010 Wiley-VCH Verlag GmbH & Co. KGaA, Weinheim

water molecules. Upon fluoride addition, the replacement of water molecules by the anions results in a decrease of the nonradiative deactivation pathways associated with OH oscillators,[4] and the luminescence properties of the complexes are largely improved.[5] The addition of fluoride anions to aqueous solutions of Ln^{III} salts can also lead to the formation of LnF_3[6] or $NaLnF_4$[7] types of nanoparticles, with large potentialities due to their interesting luminescent[8] or NMR spectroscopic relaxation[9] properties. Finally, provided one should reach the formation of strong Ln–F bonds, it may open interesting routes within the fields of ^{19}F NMR spectroscopic imaging or to the rapid and selective fixation of radioactive ^{18}F anions for positron emission tomography.[10]

The interaction of Ln^{III} complexes with fluoride anions is well documented in the literature, and it has been mainly followed by luminescence of the lanthanide cations or by ^1H NMR spectroscopy.[11,12] Furthermore, there also exist available quantitative data obtained by potentiometry.[13] These studies point to stability constants of the order of 2 to 4 log units for the association of fluoride anions to lanthanide complexes or hydrated cations.[14] Thus, positively charged Ln^{III} complexes appear to be potential candidates for the design of sensors for fluoride, a detection of particular interest due to the role of this anion in preventing dental caries, or treatment of osteoporosis.[15]

The present work aims to study the interaction of fluoride anions with $[LnL(H_2O)]Cl_3$ (Ln = Eu, Tb, and La; see Figure 1 for the chemical structure of **L**) by using a combination of absorption spectroscopy, steady-state and time-resolved luminescence spetroscopy, ^1H and ^{13}C NMR spectroscopy, and potentiometry. The data obtained by the different means are compared and rationalized using DFT calculations on the complexes and their fluoride adduct.

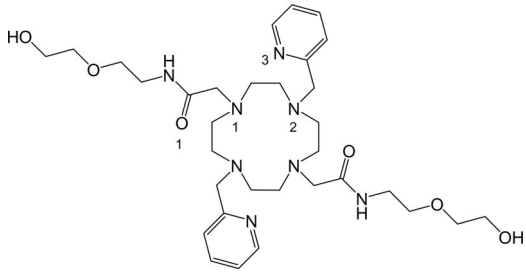

Figure 1. Ligand **L** with atom-numbering scheme.

Results and Discussion

Synthesis and Characterization of the Complexes

The $[LnL(H_2O)]Cl_3$ complexes were obtained by mixing equimolar amounts of the ligand[16] and hydrated chloride salts of the lanthanides in water, followed by precipitation of the complex in a $MeOH/Et_2O$ mixture. The isolated complexes are very hygroscopic, as evidenced by the large number of water molecules of solvation calculated from the elemental analysis. Mass spectrometry of the complexes evidenced the presence of peaks corresponding to $[LnL - 2H]^+$ and $[LnL - H]^{2+}$ species and, in the case of the Eu complex, the isotopic distribution that corresponds to the presence of the ^{151}Eu and ^{153}Eu isotopes unambiguously demonstrates the formation of the desired mononuclear complex. The IR spectra of the complexes are nearly identical, which points to a similar coordination mode for all three complexes of Eu, Tb, and La.

Protonation Constants of the Complexes

The protonation constants of the La^{III} and Eu^{III} complexes were determined by potentiometric titrations. The thermodynamic stability constants of the lanthanide complexes have not been investigated because the slow kinetics of complex formation suggest the use of batch techniques that require sample heating for extended periods to reach equilibrium; this favors amide hydrolysis in an acidic medium which, in turn, distorts pH potentiometric data. The protonation constants of the complexes are defined as in Equation (1), whereas the formation of monohydroxo complexes has been characterized by the protonation constant K_{MLOH}; see Equation (2).

$$K_{MH_iL} = \frac{[MH_iL]}{[MH_{i-1}L][H^+]} \quad (1)$$

$$K_{MLOH} = \frac{[ML]}{[ML(OH)][H^+]} \quad (2)$$

The Eu^{III} and Tb^{III} complexes present very similar properties (Table 1 and Figure 2). Both complexes undergo two protonation processes at relatively low pH (<5), most likely due to the protonation of the pyridyl groups of the ligand. At high pH both complexes experience deprotonation, likely occurring on the coordinated water molecule (see below), to form monohydroxo complexes (Figure 2).[17] The ability of $[LnL(H_2O)]^{3+}$ species to form hydroxo complexes in aqueous solution is certainly related to the high positive charge of the chelate and the presence of an inner-sphere water molecule (see below). The K_{MLOH} constant that characterizes this protonation step is slightly lower for La than for Eu. This is unexpected considering the increased charge density of the metal ion along the lanthanide series. However, a similar trend has been recently observed for cationic lanthanide complexes with a macrocyclic ligand based on a

Table 1. Protonation constants of $[LnL(H_2O)]$ complexes (Ln = Eu and La) determined by potentiometric titration.[a]

	La**L**	Eu**L**
$\log K_{MLH}$	2.67(1)	2.83(1)
$\log K_{MLH_2}$	1.99(3)	2.11(4)
$\log K_{MLOH}$	7.01(2)	7.97(2)

[a] I = 0.1 M (NaCl), T = 25 °C; numbers in parentheses are standard deviations in the last significant digit.

 © 2010 Wiley-VCH Verlag GmbH & Co. KGaA, Weinheim

1,7-diaza-12-crown-4 platform,[18] which has been attributed to a diminution of the hydration number for the small lanthanides.

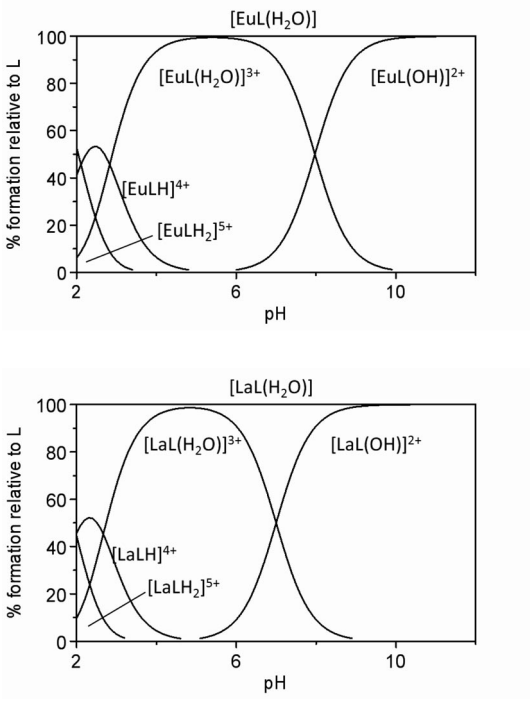

Figure 2. Species distribution diagram for the [Ln**L**(H_2O)] complexes (Ln = Eu, top; La, bottom), [**L**] = [Ln^{III}] = 1 mM, I = 0.1 M (NaCl), 25 °C.

membered chelate rings formed upon coordination of the cyclen moiety, which leads to a (δδδδ) ↔ (λλλλ) conformational change; (ii) the rotation of the pendant arms, which results in a Δ ↔ Λ configurational change. Each process alone interconverts SAP and TSAP geometries, whereas the combination of the two processes exchanges enantiomeric pairs (Figure 3).

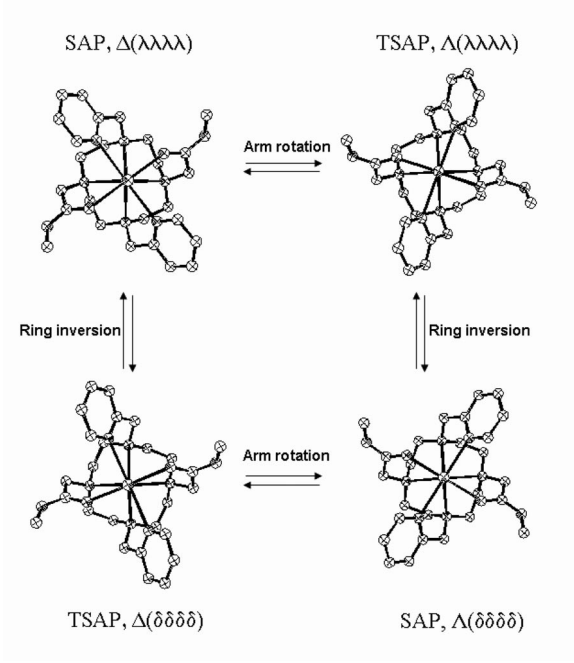

Figure 3. Optimized geometries of the four isomers of [La**L**′-$(H_2O)]^{3+}$ and their interconversion pathways. Symbols Δ and Λ refer to the helicity of the pendant arms, δ and λ to that of the macrocycle.

NMR Spectroscopic Measurements

^1H and ^{13}C NMR spectroscopic studies on the Eu and La complexes have been carried out in D_2O. Considering that the complexes are stable enough to avoid a fast exchange between the free and coordinated forms of the ligand, the different geometries usually observed for Ln^{III}–dota-like (dota = 1,4,7,10-tetraazacyclododecane-1,4,7,10-tetraacetic acid) compounds have to be considered. Figure 3 presents the four stereoisomeric forms for a [La**L**′(H_2O)] complex as obtained by DFT calculations (see below for the description of **L**′). These stereoisomers differ by the layout of the four acetate arms; they adopt either a square antiprismatic [SAP, Λ(δδδδ) or Δ(λλλλ)] or a twisted square antiprismatic [TSAP, Δ(δδδδ) or Λ(λλλλ)] geometry.[19] The two structures display a different orientation of the two square planes formed by the four cyclen nitrogen atoms and the four binding oxygen atoms (or two oxygen and two nitrogen atoms for **L**′), thereby making an angle of approximately 40° in SAP-type structures, whereas this situation is reversed and reduced to approximately –30° in TSAP-type derivatives.[20] The interconversion between the SAP and TSAP isomers has been investigated experimentally for several [Ln(dota)$(H_2O)]^-$ and Eu^{III}–dota–tetraamide complexes,[21,22] and it may proceed following two different pathways (Figure 3): (i) the inversion of the five-

The ^1H NMR spectrum of a solution of the europium complex in D_2O is extremely intricate, in part due to the low symmetry of the complex (Figure S1 in the Supporting Information). It shows up to 11 signals of similar intensity in the region from δ = 5 to 17 ppm and another 18 in the region from δ = 0 to –19 ppm. The number of signals observed would be consistent with either the presence of two major isomers of C_2 symmetry with similar populations or with the presence of a single major isomer with C_1 symmetry. Furthermore, the spectrum also shows another set of signals of lower intensity that also arises from a complex species.

The ^1H NMR spectrum of the La complex in D_2O was studied from 277 to 353 K (Figure 4). At low temperatures, the spectrum displays relatively well-resolved signals that point to the presence of a single isomer in solution with an effective C_2 symmetry. The relative populations of SAP and TSAP isomers in dota-like complexes are sensitive to numerous factors, including lanthanide ion size, the TSAP form being favored as the size of the Ln^{III} increases.[19a] For instance, the [La(dota)$(H_2O)]^{3+}$ complex is known to exist in solution almost exclusively as the TSAP isomer.[19a] Furthermore, the substitution of one of the carboxylate pendants of [Eu(dota)$(H_2O)]^{3+}$ by a pyridyl group stabilizes

 © 2010 Wiley-VCH Verlag GmbH & Co. KGaA, Weinheim

the TSAP isomer with respect to the SAP one.[23] These considerations suggest that the La^{III} complex of **L** adopts a TSAP geometry in aqueous solution. This is also supported by our DFT calculations described below.

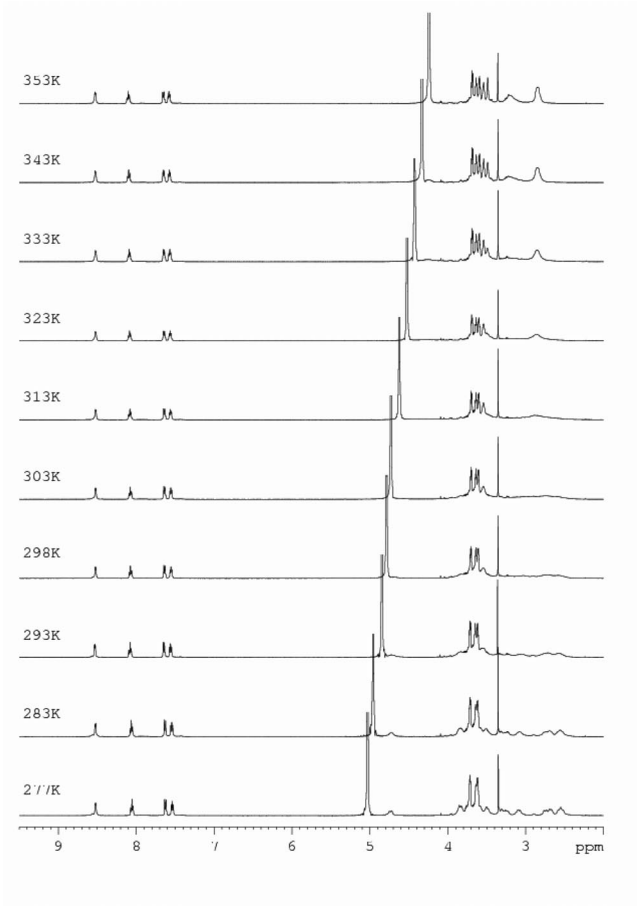

Figure 4. ^1H NMR spectrum (500 MHz) of [La**L**(H_2O)]Cl_3 in D_2O at variable temperature.

The signals due to methylenic and ethylenic protons of the ligand in the La^{III} complex gradually broaden above 277 K, thereby reflecting intramolecular conformational exchange processes (Figure 4). These signals coalesce in the temperature range 303–333 K, and above this temperature the signals sharpened. At 343 K, the proton spectrum consists of 12 signals, in agreement with an effective C_{2v} symmetry of the complex in solution. For instance, at low temperature (277 K) the methylene group linked to the pyridyl arms is observed as an AX spin system with signals at δ = 4.8 and 3.9 ppm. Coalescence of these signals is observed between 293 and 323 K, and at 343 K one resonance is observed for these protons at δ = 4.3 ppm. This observation is consistent with an arm rotation process, which leads to a $\Delta \leftrightarrow \Lambda$ interconversion. Furthermore, coalescence of the axial and equatorial protons of the macrocyclic ring is also observed, thus indicating that the ring inversion process is fast on the NMR spectroscopic timescale at high temperatures.

Considering the complexity of the ^1H spectra, we turned our attention toward the ^{13}C NMR spectrum of the complex (Figure 5). At low temperature (277 K), the aliphatic region displayed 10 peaks for the methylene carbon atoms, thereby confirming an effective C_2 symmetry of the complex under these conditions. Increasing the temperature to 298 K resulted in the broadening of the peaks between δ = 50 and 60 ppm, followed by the emergence of a single peak at high temperature (353 K), with a fortuitous isochronicity of the two peaks of the methylene groups of the cyclen ring. Since the La^{III} complex is present in solution as a single isomer, this behavior is consistent with an enantiomerization process, which interconverts the macrocyclic ring carbon atoms and represents the simple exchange between two equally populated sites. The enantiomerization process requires a combination of an arm rotation and a ring-inversion process, in line with the spectral variations observed in the ^1H NMR spectrum as a function of temperature. From the coalescence temperature of the signals due to the macrocyclic ring carbon atoms (ca. 298 K), the barrier for the enantiomerization process was estimated to be $\Delta G^{\neq}$ = (58 ± 3) kJ mol^{-1}. A nearly identical free-energy barrier is obtained from the coalescence temperature of the signals due to the methylene group linked to the pyridyl arms in the ^1H NMR spectrum (ca. 303 K). This barrier is only slightly lower than that observed for the enantiomerization process in Yb^{III}– and Lu^{III}–dota complexes.[21]

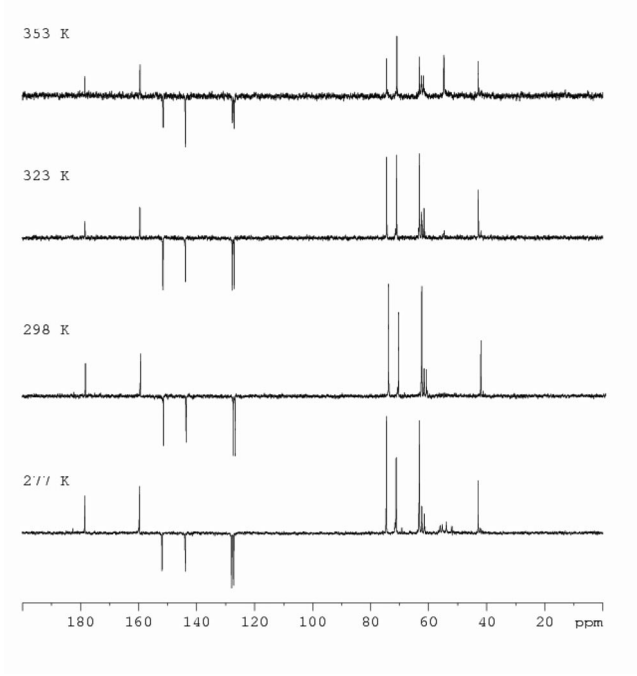

Figure 5. *J*-modulated spin-echo (JMOD) ^{13}C NMR spectra (125 MHz) of [La**L**(H_2O)]Cl_3 in D_2O at 277, 298, 323, and 353 K.

DFT Calculations

As a result of unsuccessful efforts to obtain suitable crystals of the complexes and in the absence of the corresponding experimental structural data, we aimed at obtaining structural information about the La and Eu complexes by means of density functional theory (DFT) calculations at

 © 2010 Wiley-VCH Verlag GmbH & Co. KGaA, Weinheim

the B3LYP/6-31G(d) level. On the basis of our previous experience,[24] the effective core potential (ECP) of Dolg et al. and the related [5s4p3d]-GTO valence basis set was applied in these calculations.[25] This ECP includes 46 + $4f^n$ electrons in the core for the lanthanide, thus leaving the outermost 11 electrons to be treated explicitly, which has been demonstrated to provide reliable results for several lanthanide complexes with cyclen-based ligands.[26] For computational simplicity in these calculations the [2-(2-hydroxyethoxy)ethyl] chains of the ligand were substituted by methyl groups, the methyl-substituted ligand being denoted as **L**′. Furthermore, luminescence lifetime measurements (vide infra) indicated that a single water molecule is coordinated to the Ln^{III} ion in aqueous solution. Thus, we performed our calculations on the $[Ln\mathbf{L}'(H_2O)]^{3+}$ systems. Our calculations provide the SAP and TSAP isomers as minimum energy conformations (Figure 3). The main calculated geometrical parameters for both isomers are shown in Table 2. For both the SAP and TSAP isomers our structural optimizations provide nearly undistorted C_2 symmetries, with the symmetry axis being perpendicular to the mean plane defined by the nitrogen atoms of the cyclen fragment and containing the lanthanide ion and the oxygen atom of the inner-sphere water molecules.

Table 2. Calculated geometrical parameters of the two isomers of $[Ln\mathbf{L}'(H_2O)]^{3+}$ and $[Ln\mathbf{L}'(F)]^{2+}$ complexes (Ln = La, Eu).[a]

	$[La\mathbf{L}'(H_2O)]^{3+}$		$[Eu\mathbf{L}'(H_2O)]^{3+}$		$[Eu\mathbf{L}'(F)]^{2+}$	
	SAP	TSAP	SAP	TSAP	SAP	TSAP
Ln–N1	2.845	2.860	2.758	2.785	2.872	2.922
Ln–N2	2.807	2.813	2.728	2.733	2.849	2.867
Ln–N3	2.738	2.763	2.645	2.675	2.625	2.645
Ln–O1	2.539	2.546	2.434	2.442	2.480	2.486
Ln–O_W	2.635	2.639	2.520	2.530	–	–
Ln–F	–	–	–	–	2.096	2.101
ω[b]	33.9		35.6	–21.6	35.3	–20.5
Ln–P_{N2O2}[c]	0.700	0.833	0.765	0.872	0.580	0.688
Ln–P_{N4}[d]	1.791	1.833	1.694	1.747	1.849	1.927

[a] Distances [Å] and angles [°]; see Figure 1 for atom numbering. O_W = oxygen atom of coordinated water molecules. [b] Mean twist angle [°] between the upper (P_{N2O2}, containing N3 and O1 atoms) and lower (P_{N4}, containing N1 and N2 atoms) planes. [c] Distance between the lanthanide and the P_{N2O2} least-squares plane. [d] Distance between the lanthanide and the least-squares plane defined by the amine nitrogen atoms, P_{N4}.

The distances between the Eu^{III} ion and the oxygen atoms of the amide groups are slightly longer than those observed in the solid state for dota–tetraamide complexes (2.34–2.44 Å).[27] A similar situation holds for the distances to the nitrogen atoms of the macrocyclic units, for which experimental values in dota–tetraamide complexes fall within the range 2.60–2.72 Å.[27] The distances to the amine nitrogen atoms are clearly longer in the TSAP isomer than in the SAP one. Thus, the interaction between the ligand and the donor atoms of the macrocycle appears to be weaker in the TSAP isomer than in the SAP one. The distance between the oxygen atom of the coordinated water molecule and the metal ion is approximately 0.1 Å longer than those observed in the solid state for related systems (2.41–2.44 Å),[27] but close to that normally assumed in the analysis of ^{17}O NMR spectroscopic longitudinal relaxation data of nine-coordinated Gd^{III} complexes (2.50 Å).[18] As expected, the bond lengths of the metal coordination environment are longer for the La^{III} complex than for the Eu^{III} one as a consequence of the lanthanide contraction.

The coordination polyhedron around Ln^{III} may be considered to be comprised of two virtually parallel pseudoplanes: the four amine nitrogen atoms define the lower plane (P_{N4}), whereas the oxygen atoms of the amide groups and the nitrogen atoms of the pyridyl moieties define the upper plane (P_{N2O2}). The mean twist angles ω[28] between the two parallel squares amount to approximately 36 and –22° in the SAP and TSAP isomers, respectively, in good agreement with those observed in the solid state for dota-like complexes.[20] The oxygen atom of the inner-sphere water molecule is capping the P_{N2O2} plane. The Ln^{III} ion lies closer to the P_{N2O2} plane than to the P_{N4} one, presumably due to the small cavity of the macrocyclic ligand and the harder nature of the O atoms.

The relative free energy of the SAP isomer with respect to the TSAP one calculated for the La^{III} complex amounts to 3.77 kcal mol^{-1}. Calculations thus confirm that the single isomer observed in solution for the La^{III} complex corresponds to the TSAP form (see above). For the Eu^{III} complex, this relative free energy is reduced to 2.29 kcal mol^{-1}, in line with the progressive stabilization of the SAP isomer observed for Ln^{III}–dota complexes upon decreasing the ionic radius of the metal ion across the lanthanide series.[19a]

Spectrophotometric Characterization of the Complexes

The UV/Vis absorption spectra of the Eu and Tb complexes are dominated by the $\pi \rightarrow \pi^*$ transitions centered on the pyridyl rings,[29] observed at 263 nm for both complexes (Figure S2 in the Supporting Information). Upon excitation into this absorption band, both complexes displayed the typical emission spectra associated with the characteristic emission of *f*–*f* transitions (Figure 6). For the Tb complexes, emission bands corresponding to the $^5D_4 \rightarrow {}^7F_J$ transitions are observed with maxima at 484 (J = 6), 539 (J = 5), 579 (J = 4), and 614 nm (J = 3), whereas J = 2 to 0 transitions are only faintly observed above 630 nm. It is worth noting that a remarkable feature of the spectrum lies in the relatively weak intensity of the $^5D_4 \rightarrow {}^7F_5$ transition, which amounts to 43% of the total emitted intensity (respectively, 41, 12, and 3% for J = 6, 4, and 3). Although it is generally observed that this transition is by far the most intense,[30] the relative intensity is here almost the same as that of the $^5D_4 \rightarrow {}^7F_6$ transition, a feature also observed in other cyclen-based luminescent Tb complexes with C_4 symmetry.[31]

The emission spectrum of the Eu complex is also characteristic of the *f*–*f* transitions of europium, with $^5D_0 \rightarrow {}^7F_J$ transitions observed at 574 (J = 0), 580–598 (max. at 589, J = 1), 599–630 (max. at 612, J = 2), 647 (J = 3), and 672–700 nm (max. at 692 nm, J = 4). The observation of only two sublevels for the $^5D_0 \rightarrow {}^7F_1$ transition, together with

 © 2010 Wiley-VCH Verlag GmbH & Co. KGaA, Weinheim

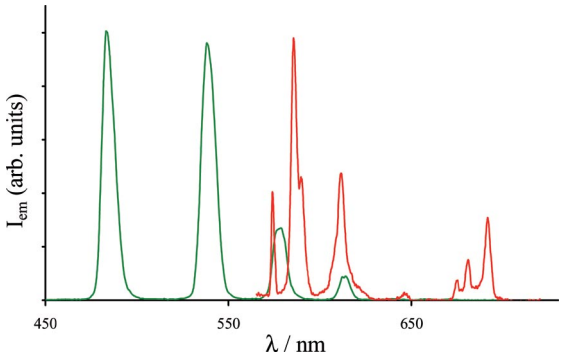

Figure 6. Emission spectra of [Tb**L**(H_2O)]Cl_3 (green, λ_{exc} = 230 nm) and [Eu**L**(H_2O)]Cl_3 (red, λ_{exc} = 250 nm) in 0.01 M TRIS/$HClO_4$, pH = 7.0 (normalized on the maxima of emission).

the very low relative intensity of the hypersensitive $^5D_0 \rightarrow {}^7F_2$ transition compared with $^5D_0 \rightarrow {}^7F_1$ (I_2/I_1 = 0.63) point to a high symmetry of the ligand field around the europium cation,[32] in contrast to the low C_2 symmetry observed by ^1H NMR spectroscopy for the La complex. Such a high symmetry should appear surprising with regards to the chemical structure of the ligand. Nevertheless, it must not be directly related to the chemical structure, but rather more to the ligand-field effect of each coordinating atom. Considering that the nephelauxetic parameters attributed to N-heterocyclic atoms of the pyridyl rings and O-amide atoms of the amide functions are very similar (δ = –15.3[33] and –15.7 ppm,[34] respectively, for N and O), the ligand-field effects exerted by these are related by a quasi-C_4 symmetry axis passing through the Eu atom and perpendicular to the tetraazamacrocyclic frame. For both complexes, the time dependence of the intensity decay can be perfectly fitted with a monoexponential function in water, D_2O, or buffered 0.01 M tris(hydroxymethyl)aminomethane (TRIS)/$HClO_4$ aqueous solution (Table 3).

Table 3. Spectroscopic properties of the Eu and Tb complexes.

	[Eu**L**(H_2O)]Cl_3	[Tb**L**(H_2O)]Cl_3
λ_{max} [nm] (ε [$M^{-1}cm^{-1}$])[a]	266 (6580)	266 (6050)
Φ_{ov} [%][a,b]	0.11	0.68
τ (H_2O) [μs]	545	1690
τ (TRIS/$HClO_4$)[c] [μs]	549	1670
τ (D_2O) [μs]	1790	2910

[a] Pure water. [b] Estimated relative error ±15%. [c] 0.01 M, pH = 7.0.

The data reported in Table 3 show that the buffer has little influence on the luminescence lifetimes in water, as expected with the use of the weakly coordinating perchlorate anion. Using the methodology developed by Horrocks and co-workers[4b] with corrections for the second-sphere interactions[4a,35] (see Exp. Section), one obtains hydration numbers of 1.1 for Eu and 1.0 for Tb, in agreement with a coordination number of 9 for both cations, provided by the water molecule and the eight coordination sites of the ligand. The overall luminescence quantum yields of the complexes were measured in water and were found to be rather weak, but in agreement with values of the literature.[31] Considering the clear distribution of the different *f*–*f* transitions in the emission spectrum of the Eu complex, it was possible to estimate the europium-centered luminescence quantum yield, Φ_{Eu}. The calculation of Φ_{Eu} is based on the assumption that the $^5D_0 \rightarrow {}^7F_1$ transition of europium has no electric dipole contribution, that its energy and dipole strength are constant, and that the contributions of $^5D_0 \rightarrow {}^7F_{5,6}$ are negligible.[36] The emission spectrum can then be correlated to the radiative lifetime of Eu, τ_{rad}, by the formula in Equation (3).[37]

$$\frac{1}{\tau_{rad}} = k_{rad} = A_{0\rightarrow1}\frac{\hbar\omega_{0\rightarrow1}}{S_{0\rightarrow1}}\sum_{J=0}^{4}\frac{S_{0\rightarrow J}}{\hbar\omega_{0\rightarrow J}} \quad (3)$$

$A_{0\rightarrow1}$ is Einstein's coefficient for spontaneous emission probability for the $^5D_0 \rightarrow {}^7F_1$ transition (50 s^{-1}), $\hbar\omega_{0\rightarrow J}$ is the energy of the $^5D_0 \rightarrow {}^7F_J$ transition, and $S_{0\rightarrow J}$ is the integrated emission of the $^5D_0 \rightarrow {}^7F_J$ bands. The radiative lifetime can then be linked to the Eu-centered luminescence quantum yield and to the overall luminescence quantum yield by Equations (4) and (5).

$$\Phi_{Eu} = \tau_{obs}/\tau_{rad} \quad (4)$$

$$\Phi_{ov} = \eta_{sens} \times \Phi_{Eu} \quad (5)$$

τ_{obs} is the observed luminescence lifetime and η_{sens} the sensitization efficiency of the antenna ligand. Calculations led to a radiative lifetime of 7.70 ms, a 7.1% europium-centered quantum yield with a sensitization efficiency of only 1.6%, thus showing that the poor quantum yield is due both to a poor sensitization, attributed to a large energy gap between the ligand-centered excited states and the europium $^5D_{0,1}$ states,[38] and to a modest europium-centered luminescence efficiency, which result from deactivation from OH oscillators of the water molecule, and also for a non-negligible part from CH and NH ones (vide infra).

Interaction of the Europium and Terbium Complexes with F^-, Cl^-, and Br^- Anions

The interaction of the complexes with halide anions was first studied by means of absorption and luminescence spectroscopy. For both Eu and Tb complexes, the absorption and luminescence changes were monitored as a function of the concentration of added anions in a TRIS/$HClO_4$ buffer (0.01 M, pH = 7.0). In all cases, the changes in the absorption spectra were very weak and did not provide any evidence of anion coordination. Similarly, for both Cl^- and Br^- anions, no changes could be observed in the luminescence spectra up to 1000 equiv. of added anions, pointing to a weak interaction of these anions.[39] In contrast, the addition of fluoride anions led to important changes in the shape and intensity of the luminescence spectra (Figure 7).

 © 2010 Wiley-VCH Verlag GmbH & Co. KGaA, Weinheim

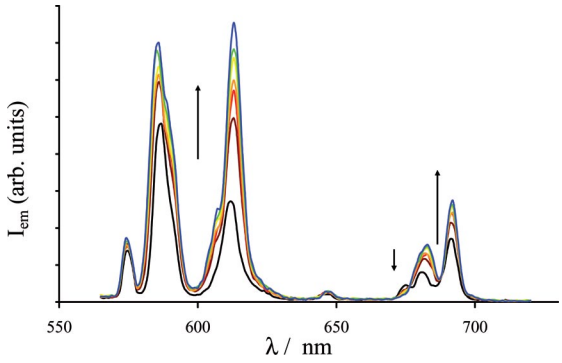

Figure 7. Evolution of the emission spectra of a 4.2×10^{-5} M solution of [Eu**L**(H_2O)]Cl_3 in 0.01 M TRIS/$HClO_4$ buffer (pH = 7.0) upon addition of 0 (black), 30 (brown), 60 (red), 120 (orange), 240 (yellow), 600 (green), and 1200 (blue) equiv. of NaF (λ_{exc} = 245 nm, corrected for dilution, $[F^-]_{added}$ = 0.5 M).

The overall emitted intensity gradually increases, and one can notice that the relative intensity of the $^5D_0 \rightarrow {}^7F_2$ and $^5D_0 \rightarrow {}^7F_1$ transitions also increases reaching a ratio of 0.92. It has been demonstrated that the nature and polarizability of the group that occupies a position on or close to the principal axis of the complex affects the relative intensity of the $^5D_0 \rightarrow {}^7F_2$ transition.[40] The more polarizable the axial donor atom is, the greater the relative intensity of the $^5D_0 \rightarrow {}^7F_2$ emission band. Thus, the increase of the relative intensity of the $^5D_0 \rightarrow {}^7F_2$ transition is attributed to the substitution of a coordinated water molecule by a more polarizable F^- anion. Interestingly, important changes could also be observed within the shape of the $^5D_0 \rightarrow {}^7F_4$ transition; the high-energy component present at 675 nm disappears in the spectra of the fluoride adduct. The evolution of the emission spectra was then fitted with the Specfit software.[41] The factorial analysis revealed the presence of only two species and the changes were fitted according to Equation (6).

$$[Eu\mathbf{L}(H_2O)]^{3+} + F^- \leftrightarrow [Eu\mathbf{L}F]^{2+} + H_2O \quad (6)$$

Since the concentration of solvent water is effectively constant, the apparent equilibrium constant corresponding to Equation (6) may be written as Equation (7).

$$K = \frac{[(Eu\mathbf{L}F)^{2+}]}{[(Eu\mathbf{L}^{3+}][F^-]} \quad (7)$$

A $\log K$ value of (2.86 ± 0.06) was obtained. The evolution of the species formed during the titration and the calculated spectrum of the [Eu**L**$(H_2O)]^{3+}$ and [Eu**L**F$]^{2+}$ species are presented in Figures S3 and S4 in the Supporting Information.

During titration, the addition of fluoride anions also resulted in an increase of the luminescence lifetime observed for Eu; at the end of the titration, this lifetime reached 1.07 ms. Furthermore, by fixing lifetime values of 0.56 and 1.07 in the fitting process for the water and fluoride ternary species, respectively, all decay curves corresponding to the intermediate points could be perfectly fitted.

The reconstituted luminescence spectra (Figure S4 in the Supporting Information) allowed calculation of the overall luminescence quantum yield of the [Eu**L**F$]^{2+}$ species relative to its water precursor, thus giving a value of 0.20%. Similarly to what was done for [Eu**L**$(H_2O)]^{3+}$ (vide supra), the emission spectrum at medium resolution (5 Å; Figure S5 in the Supporting Information) was used to calculate the radiative lifetime (7.2 ms), the metal-centered luminescence quantum yield (15%), and the sensitization efficiency (1.35%). It is thus clear that the replacement of the water molecule by a fluoride anion has little impact on the radiative lifetime of the species, but doubles the metal-centered luminescence efficiency by removing the nonradiative deactivation pathways associated with the OH oscillators. Unfortunately, the replacement has little if any impact on the sensitization efficiency, which remains poor for both complexes.

The binding of F^- was also investigated by using DFT calculations. The main geometrical parameters calculated for the SAP and TSAP isomers of [Eu**L**′(F)$]^{2+}$ are shown in Table 2. The coordination of the F^- anion induces important changes in the bond lengths of the metal coordination environment. Indeed, anion coordination causes an important lengthening of the distances to the nitrogen atoms of the macrocycle (ca. 0.11–0.14 Å). The distances to the oxygen atoms of the amide groups increase by approximately 0.04 Å, presumably due to the electrostatic repulsion between these donor atoms and the coordinated anion. Anion coordination brings the metal ion closer to the P_{N2O2} plane, whereas the distance to the P_{N4} plane increases. We want to highlight that these relatively pronounced changes in the metal coordination environment upon anion binding are in part due to the fact that our calculations were performed in the gas phase, in which electrostatic interactions between the cationic complex and the anion are expected to play a more important role than in solution. The calculated Eu–F distances (ca. 2.10 Å) are approximately 0.09 Å shorter than those observed in the solid state for nine-coordinated Eu^{III} complexes that contain terminal F^- ligands,[42] which is again attributed to the important role that electrostatic interactions play in gas-phase calculations. Our calculations provide a relative free energy of the SAP form with respect to the TSAP of 2.39 kcal mol^{-1} (2.29 kcal mol^{-1} for [Eu**L**′$(H_2O)]^{3+}$, see above). Thus, we conclude that F^- binding does not affect substantially the relative stability of the SAP and TSAP isomers, the TSAP form being the most stable one for both [Eu**L**$(H_2O)]^{3+}$ and [Eu**L**(F)$]^{2+}$ complexes.

The interactions of fluoride anions with the lanthanide complexes (Ln = La, Eu) have also been investigated with respect to the stability of the complex by means of potentiometric titrations. The analysis of the titration curves provided logarithmic values for the complexation constants [Equation (7)], of 3.42(5) (La) and 3.47(4) (Eu). These values were found to be relatively close to those obtained by spectrophotometric titrations. The different experimental conditions used for the two methods (0.1 M NaCl for potentiometry and 0.01 M TRIS/$HClO_4$ for spectroscopy) may

 © 2010 Wiley-VCH Verlag GmbH & Co. KGaA, Weinheim

be partly responsible for the differences observed. No evidence for the coordination of F^- to protonated forms of the complexes was obtained from the fitting of the titration data. However, this is expected considering the pK_a of HF (3.20[43]), as at low pH values in which protonated forms of the complexes are formed most of the fluoride is present in solution as FH_{aq}. Figure 8 illustrates the distribution of the species formed during the potentiometric titration of the Eu complex in the presence of 1 equiv. of fluoride anions. The ternary complex species $[Eu\mathbf{L}(F)]^{2+}$ is the major species in solution in the pH range 3.6–8.1. Above pH 8.1 the monohydro complex predominates in solution, whereas below pH ≈ 4 the concentration of ternary species diminishes due to the protonation of F^-. A comparison of the speciation diagrams calculated for the Eu^{III} complex in the absence (Figure 2) and in the presence (Figure 8) of equimolar F^- shows that F^- competes with OH^- for the coordination to the lanthanide ion. For instance, in the absence of F^-, 51.7% of the complex is in the form of $[Eu(\mathbf{L})(OH)]^{2+}$ at pH 8.0, whereas in the presence of F^-, the amount of the hydroxide complex at this pH represents only 29.9% of the total Eu^{III}.

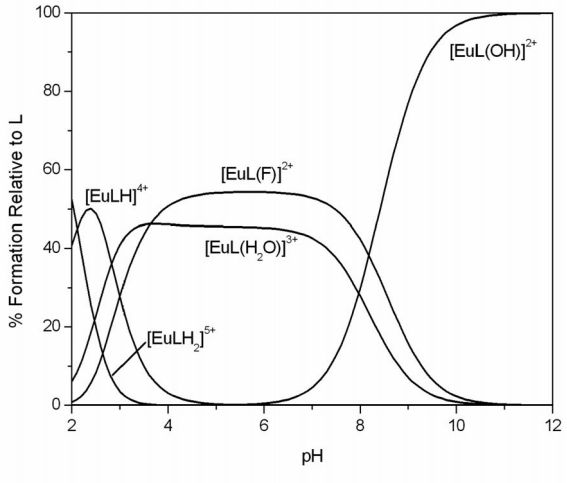

Figure 8. Distribution diagram of the species formed upon potentiometric titration of an equimolar mixture of $[Eu\mathbf{L}(H_2O)]Cl_3$ and F^- anions $[Eu^{3+}] = [\mathbf{L}] = [F^-] = 1$ mM, $I = 0.1$ M (NaCl), 25 °C.

Conclusion

The interaction of fluoride anions with triply charged lanthanide complexes based on dota-like ligands can be monitored by various spectroscopic and potentiometric means. It reveals a very selective interaction, compared with chloride or bromide anions, but nevertheless with a medium to weak affinity constant. This selectivity may be attributed to the hard nature of the F^- ligand, which results in a stronger interaction with hard Lewis acids such as the Ln^{III} ions. However, the size of the anion (1.33, 1.81, and 1.96 Å for F^-, Cl^-, and Br^-, respectively) could also play an important role in the observed selectivity. The fluoride anion can displace the apical water molecule in the complex without major perturbation of the coordination sphere, as evidenced by DFT calculations. On the other hand, this exchange resulted in dramatic changes in the luminescence spectrum of the Eu complex, due to the substitution of a coordinated water molecule by a more polarizable F^- anion. It is worth noting that these results represent an encouraging entry into the field of fluoride sensing in aqueous solution, provided that the interaction should be strengthened, as, for example, by the introduction of supplementary hydrogen-bonding interactions able to further stabilize the fluoride anion in its apical position. Current efforts are directed toward this goal.

Experimental Section

UV/Vis absorption spectra were recorded with a Varian Cary 300 spectrometer. Emission and excitation spectra were recorded with a PTI Quantamaster spectrometer. Luminescence decays were obtained with the same instrument over temporal windows covering at least five decay times. Luminescence quantum yields were measured with a Perkin–Elmer LS50B spectrometer working in the phosphorescence mode (delay of 0 μs, 10 ms integration windows) according to conventional procedures,[44] with diluted solutions (optical density <0.05), using $[Ru(bipy)_3]Cl_2$ (bipy = 2,2′-bipyridine) in nondegassed water (Φ = 2.8%),[45] or rhodamine 6G in ethanol (Φ = 88%)[46] as references for Eu and Tb, respectively, with the necessary correction for the refractive index of the media used.[47] Estimated errors are ±15%. Hydration numbers, q, were obtained using Equation (8), in which τ_{H_2O} and τ_{D_2O} refer to the measured luminescence decay lifetime (in ms) in water or deuterated water, respectively, using A = 1.11 and B = 0.31[35] for Eu, and A = 5.0 and B = 0.06 for Tb.[4a]

$$q = A \times (1/\tau_{H_2O} - 1/\tau_{D_2O} - B) \quad (8)$$

Inductively coupled plasma atomic emission spectroscopy (ICP-AES) analyses of dissolved samples in water were performed with a Varian 720 spectrometer equipped with a quartz Meinhard nebulizer and a cyclone spray chamber. Eu and Tb emission was measured at 381.967 and 350.917 nm, respectively. Calibration of the instrument was done with standards prepared from 1000 mg L^{-1} certified standards (CPI International). ^1H and ^{13}C NMR spectra were recorded with Avance 500 Bruker (500 MHz) equipped with a 5 mm cryoprobe (TCI $^1H/^{13}C/^{15}N$), Avance 400 Bruker (400 MHz), or AMX-3 300 Bruker (300 MHz) spectrometers using MeOH as internal reference. 2D $^1H,^1H$ homonuclear and $^1H,^{13}C$ heteronuclear correlations, and homonuclear decoupling experiments permitted the full assignation of the ^1H and ^{13}C signals.

Synthesis of the Complexes, General Procedure: Ligand **L**[16] (1 equiv.) was dissolved in deionized water (25 mL) and $LnCl_3 \cdot 6H_2O$ (1 equiv.) was added. The solution was agitated overnight at room temp. and the solvents evaporated to dryness. The oily residue was dissolved in a minimal amount of MeOH (ca. 1 mL) and precipitated by addition of diethyl ether. The mother liquors were separated, the oily residue was dissolved in MeOH, and the solvents evaporated to dryness, which led to a transparent glassy film from which the complex was isolated by trituration with Et_2O and drying under vacuum. The isolated compounds are highly hygroscopic upon exposure to air.

$[EuL(H_2O)]Cl_3 \cdot 8H_2O$: 220 mg (78% yield) from 170 mg of **L**. $C_{32}H_{54}Cl_3EuN_8O_7 \cdot 8H_2O$ (921.15 + 144.08): calcd. C 36.08, H 6.62,

 © 2010 Wiley-VCH Verlag GmbH & Co. KGaA, Weinheim

N 10.52; found C 36.58, H 6.20, N 10.02. ICP-AES on dried sample: calcd. (%) for Eu, 16.5; found 16.8 (4). MS (ES^+, H_2O): *m*/*z* (%) = 793.6 (<1) $[EuL - 2H]^+$, 795.6 (<1) $[EuL - 2H]^+$, 398.5 (15) $[EuL - H]^{2+}$, 265.8 (24) $[EuL^{3+}]$. IR (ATR): 3354 (br. s), 2978 (w), 2944 (w), 2872 (w), 1626 (s), 1604 (m), 1442 (m), 1311 (m), 1124 (m), 1077 (m), 1007 (m), 967 (w), 888 (w) cm^{-1}.

$[TbL(H_2O)]Cl_3·9.5H_2O$: 91 mg (62% yield) from 85 mg of **L**. $C_{32}H_{54}N_8O_7TbCl_3·9.5H_2O$ (926.24 + 153.11): calcd. C 34.96, H 6.69, N 10.19; found C 34.57, H 6.19, N 9.93. ICP-AES on dried sample: calcd. (%) for Tb, 17.1; found 17.7 (4). MS (ES^+, MeOH): *m*/*z* (%) = 801.7 (9) $[TbL - 2H]^+$, 401.6 (100) $[TbL - H]^{2+}$, 323.4 (43) $[TbL - H]^{2+}$. IR (ATR): 3250 (br. s), 2937 (w), 2874 (w), 1629 (s), 1605 (m), 1446 (m), 1299 (m), 1124 (m), 1077 (m), 1015 (w), 1001 (w), 974 (w), 887 (w) cm^{-1}.

$[LaL(H_2O)]Cl_3·7H_2O$: 83 mg (59% yield) from 85 mg of **L**. $C_{32}H_{54}Cl_3LaN_8O_7·7H_2O$ (908.7 + 126.03): calcd. C 37.16, H 6.63, N 10.83; found C 37.17, H 6.19, N 10.48. IR (ATR): 3354 (br. s), 2944 (w), 2871 (w), 1626 (s), 1604 (m), 1442 (m), 1311 (m), 1124 (m), 1077 (m), 1007 (m), 967 (w), 888 (w) cm^{-1}. ^1H NMR (D_2O, 300 MHz, 353 °C): δ = 2.85 (m, 8 H, -CH_2-*N*-CH_2-CO), 3.23 (m, 8 H, -CH_2-*N*-CH_2-Py), 3.48 (d, ^2J = 16 Hz, 4 H, -CH_2-CO-), 3.58 (m, 4 H, -NH-CH_2-CH_2-O-), 3.60 (m, 4 H, -CH_2-CH_2-OH), 3.62 (m, 4 H, -CH_2-CH_2-O-), 3.67 (m, 4 H, -CH_2-CH_2-OH), 4.24 (m, 4 H, -CH_2-Py), 7.61 (t, ^3J = 8 Hz, 2 H, H_{Py}), 7.92 (d, ^3J = 8 Hz, 2 H, *HPy*), 8.23 (t, ^3J = 8 Hz, 2 H, *H*Py), 8.31 (d, ^3J = 4 Hz, 2 H, *H*Py) ppm. ^{13}C NMR (D_2O, 75.48 MHz, 353 °C): δ = 43.3 (CH_2-NH-CO), 54.6, 55.2 (CH_2-N ring), 62.2 (N-CH_2-Py), 62.9 (N-CH_2-CO), 63.6 (CH_2-OH), 71.3 (CH_2-O), 74.8 (CH_2-O), 127.5, 128.0, 144.3, 151.9, 159.8 (Py), 178.9 (CO-NH) ppm.

Computational Methods: All calculations were performed by employing hybrid DFT with the B3LYP exchange-correlation functional,[48] and the Gaussian 03 package (revision C.01).[49] For computational simplicity in these calculations, the *N*-[2-(2-hydroxyethoxy)ethyl]acetamide chains of **L** were substituted by methyl groups, the methyl-substituted ligand being denoted as **L′**. Full geometry optimizations of the $[LnL'(H_2O)]^{3+}$ (Ln = La, Eu) and $[EuL'(F)]^{2+}$ systems were performed in vacuo by using the 6–31G(d) basis set for the ligand atoms. Different computational studies on Ln^{III} complexes have shown that the 4f orbitals do not participate in bonding because of their contraction into the core.[50] As a consequence, no effect of the spin–orbital coupling on the equilibrium geometries of Ln^{III} complexes was found.[51] Thus, spin–orbit effects were not taken into account in the present work. Relativistic effects were considered through the use of relativistic effective core potentials (RECP). Therefore, for the lanthanides the quasirelativistic effective core potential (ECP) of Dolg et al. and the related [5s4p3d]-GTO valence basis was applied.[25] This ECP treats $[Kr]4d^{10}4f^n$ as fixed cores, whereas the remaining electrons are treated explicitly. Compared with all-electron basis sets, ECPs account to some extent for relativistic effects, which are believed to become important for the elements from the fourth row of the periodic table. The stationary points found on the potential-energy surfaces as a result of the geometry optimizations have been tested to represent energy minima rather than saddle points by means of frequency analysis. The relative free energies of the SAP and TSAP isomers were calculated in vacuo at the B3LYP/6-31G(d) level, including non-potential-energy contributions (zero-point energies and thermal terms) obtained through frequency analysis.

Potentiometric Titration: Potentiometric measurements were performed in a jacketed cell thermostatted at 25.0 °C, kept under an inert atmosphere of purified argon, with an automatic titrator (Metrohm, DMS Titrino 716) connected to a microcomputer. The free hydrogen concentrations were measured with a glass Ag/AgCl combined electrode (Metrohm) filled with 0.1 M NaCl. The electrode was calibrated to read –log[H^+], designated as p[H], by titration of a small quantity of diluted HCl by standardized NaOH at 0.02 M ionic strength and at 25.0 °C (and determining the equivalent point by Gran's method)[52] followed by adjustment of the pH meter so as to minimize the calculated p[H] versus observed values. A logK_w for the system, defined in terms of log([H^+][OH^-]), was found to be –13.78 at the ionic strength employed and was maintained fixed during refinements.[52]

Protonation Constants of the Lanthanide Complexes and Ternary Complex Formation: Potentiometric measurements of a solution containing the complexes were prepared at approximately 1 mM concentration with ionic strength I = 0.10 M (NaCl). Each titration used at least 10 points per neutralization of a hydrogen ion equivalent and titrations were repeated until a satisfactory agreement was reached. A minimum of three sets of data were used in each case to calculate the overall protonation constants and their standard deviations. The range of accurate p[H] measurements was considered to be 2–12. Potentiometric titrations of the La^{III} and Eu^{III} complexes of **L** were also performed in the presence of 1 equiv. of F^- salt (introduced as NaF) to determine the stability constants of the corresponding ternary complexes. Equilibrium constants and species distribution diagrams were calculated by using the program HYPERQUAD 2003.[53]

Supporting Information (see footnote on the first page of this article): ^1H NMR spectrum of the Eu^{III} complex, absorption spectra of the Eu^{III} and Tb^{III} complexes, evolution of the species formed during the titration of the Eu^{III} complex with F^-, calculated emission spectra of the $[EuL(H_2O)]^{3+}$ and $[EuLF]^{2+}$ species, 500 MHz ^1H,^1H NMR COSY, ^1H,^{13}C NMR HMBC, and NMR HMQC spectra of $[LaL(H_2O)]Cl_3$ in D_2O at 277 K, and optimized Cartesian coordinates for the $[LnL'(H_2O)]^{3+}$ (Ln = La, Eu) and $[EuL'(F)]^{2+}$ systems.

Acknowledgments

The authors thank the "service commun" of NMR facilities of the University of Brest and are indebted to Centro de Supercomputación de Galicia (CESGA) for providing the computer facilities. This research was performed within the framework of the EU COST Action D38 "Metal-Based Systems for Molecular Imaging Applications."

[1] G. R. Choppin, *J. Alloys Compd.* **2002**, *344*, 55–59.
[2] a) N. Sabbatini, S. Perathoner, G. Lattanzi, S. Dellonte, V. Balzani, *J. Phys. Chem.* **1987**, *91*, 6136–6139; b) B. Alpha, J.-M. Lehn, G. Mathis, *Angew. Chem. Int. Ed. Engl.* **1987**, *26*, 266–267; c) J. P. Cross, A. Dadabhoy, P. G. Sammes, *J. Lumin.* **2004**, *110*, 113–124.
[3] H. Bazin, M. Préaudat, E. Trinquet, G. Mathis, *Spectrochim. Acta, Part A* **2001**, *57*, 2197–2211.
[4] a) A. Beeby, I. M. Clarkson, R. S. Dickins, S. Faulkner, D. Parker, L. Royle, A. S. De Sousa, J. A. G. Williams, M. Woods, *J. Chem. Soc. Perkin Trans. 2* **1999**, 493–504; b) W. deW. Horrocks Jr., D. R. Sudnick, *J. Am. Chem. Soc.* **1979**, *101*, 334–340.
[5] L. J. Charbonnière, N. Hildebrandt, R. Ziessel, H.-G. Löhmannsröben, *J. Am. Chem. Soc.* **2006**, *128*, 12800–12809.
[6] a) P. R. Diamente, F. C. J. M. van Veggel, *J. Fluoresc.* **2005**, *15*, 543–551; b) F. Wang, Y. Zhang, X. Fan, M. Wang, *Nanotechnology* **2006**, *17*, 1527–1532; c) S. Sivakumar, F. C. J. M. van Veggel, P. S. May, *J. Am. Chem. Soc.* **2007**, *129*, 620–625.
[7] L. Wang, Y. Li, *Chem. Mater.* **2007**, *19*, 727–734.

 © 2010 Wiley-VCH Verlag GmbH & Co. KGaA, Weinheim

[8] a) J.-C. Boyer, F. Vetrone, L. A. Cuccia, J. A. Capobianco, *J. Am. Chem. Soc.* **2006**, *128*, 7444; b) S. Sivakumar, P. R. Diamente, F. C. J. M. van Veggel, *Chem. Eur. J.* **2006**, *12*, 5878–5884; c) L. J. Charbonnière, J.-L. Rehspringer, R. Ziessel, Y. Zimmermann, *New J. Chem.* **2008**, *32*, 1055–1059.
[9] F. Evanics, P. R. Diamente, F. C. J. M. van Veggel, G. J. Stanisz, R. S. Prosser, *Chem. Mater.* **2006**, *18*, 2499–2505.
[10] S. M. Ametamey, M. Honer, P. A. Schubiger, *Chem. Rev.* **2008**, *108*, 1501–1516.
[11] For recent examples, see: a) C. M. G. dos Santos, T. Gunnlaugsson, *Dalton Trans.* **2009**, 4712–4721; b) Y. Kataoka, P. Dharam, H. Miyake, S. Shinoda, H. Tsukube, *Dalton Trans.* **2007**, 2784–2791; c) H. Tsukube, Y. Suzuki, D. Paul, Y. Kataoka, S. Shinoda, *Chem. Commun.* **2007**, 2533–2535; d) H. Tsukube, T. Yamada, S. Shinoda, *J. Alloys Compd.* **2004**, *374*, 40–45; e) M. Montalti, L. Prodi, N. Zaccheroni, L. Charbonnière, L. Douce, R. Ziessel, *J. Am. Chem. Soc.* **2001**, *123*, 12694–12695; f) Y. Kataoka, D. Paul, H. Miyake, T. Yaita, E. Miyoshi, H. Mori, S. Tsukamoto, H. Tatewaki, S. Shinoda, H. Tsukube, *Chem. Eur. J.* **2008**, *14*, 5258–5266; g) D. Zhang, M. Shi, Z. Liu, F. Li, T. Yi, C. Huang, *Eur. J. Inorg. Chem.* **2006**, 2277–2284; h) R. S. Dickins, S. Aime, A. S. Batsanov, A. Beeby, M. Botta, J. I. Bruce, J. A. K. Howard, C. S. Love, D. Parker, R. D. Peacock, H. Puschmann, *J. Am. Chem. Soc.* **2002**, *124*, 12697–12705; i) C. G. Gulgas, T. M. Reineke, *Inorg. Chem.* **2008**, *47*, 1548–1559; j) L. J. Charbonnière, R. Ziessel, M. Montalti, N. Zaccheroni, C. Boehme, G. Wipff, *J. Am. Chem. Soc.* **2002**, *124*, 7779–7788; k) H. Tsukube, A. Onimaru, S. Shinoda, *Bull. Chem. Soc. Jpn.* **2006**, *79*, 725–730; l) P. Atkinson, Y. Bretonniere, D. Parker, G. Muller, *Helv. Chim. Acta* **2005**, *88*, 391–405; m) T. Yamada, S. Shinoda, H. Tsukube, *Chem. Commun.* **2002**, 1218–1219.
[12] For reviews on anion sensing with lanthanide complexes, see: a) D. Parker, *Coord. Chem. Rev.* **2000**, *205*, 109–130; b) H. Tsukube, S. Shinoda, *Chem. Rev.* **2002**, *102*, 2389–2403.
[13] a) E. L. Yee, O. A. Gansow, M. J. Weaver, *J. Am. Chem. Soc.* **1980**, *102*, 2278–2285; b) R. M. Scarborough Jr., A. B. Smith, *J. Am. Chem. Soc.* **1977**, *99*, 7087–7089.
[14] Y. R. Luo, R. H. Byrne, *J. Solution Chem.* **2007**, *36*, 673–689.
[15] a) X. Peng, Y. Wu, J. Fan, M. Tian, K. Han, *J. Org. Chem.* **2005**, *70*, 10524–10531; b) H. J. Kim, S. K. Kim, J. Y. Lee, J. S. Kim, *J. Org. Chem.* **2006**, *71*, 6611–6614.
[16] J. F. Morfin, M. Lebaccon, R. Tripier, H. Handel, *Polyhedron* **2009**, *28*, 3691–3698.
[17] A. Nonat, P. H. Fries, J. Pecaut, M. Mazzanti, *Chem. Eur. J.* **2007**, *13*, 8489–8506.
[18] Z. Palinkas, A. Roca-Sabio, M. Mato-Iglesias, D. Esteban-Gomez, C. Platas-Iglesias, A. de Blas, T. Rodriguez-Blas, E. Toth, *Inorg. Chem.* **2009**, *48*, 8878–8889.
[19] a) S. Aime, M. Botta, M. Fasano, M. P. M. Marques, C. F. G. C. Geraldes, D. Pubanz, A. E. Merbach, *Inorg. Chem.* **1997**, *36*, 2059–2068; b) S. Hoeft, K. Roth, *Chem. Ber.* **1993**, *126*, 869–873; c) S. Aime, M. Botta, G. Ermondi, *Inorg. Chem.* **1992**, *31*, 4291–4299.
[20] D. Parker, R. S. Dickins, H. Puschmann, C. Crossland, J. A. K. Howard, *Chem. Rev.* **2002**, *102*, 1977–2010.
[21] a) V. Jacques, J. F. Desreux, *Inorg. Chem.* **1994**, *33*, 4048–4053; b) S. Aime, A. Barge, M. Botta, M. Fasano, J. D. Ayala, G. Bombieri, *Inorg. Chim. Acta* **1996**, *246*, 423–429.
[22] M. Woods, S. Aime, M. Botta, J. A. K. Howard, J. M. Moloney, M. Navet, D. Parker, M. Port, O. Rousseaux, *J. Am. Chem. Soc.* **2000**, *122*, 9781–9792.
[23] S. Aime, A. S. Batsanov, M. Botta, J. A. K. Howard, M. P. Lowe, D. Parker, *New J. Chem.* **1999**, *23*, 669–670.
[24] a) L. Charbonnière, S. Mameri, P. Kadjane, C. Platas-Iglesias, R. Ziessel, *Inorg. Chem.* **2008**, *47*, 3748–3762; b) M. Mato-Iglesias, T. Rodriguez-Blas, C. Platas-Iglesias, M. Starck, P. Kadjane, R. Ziessel, L. Charbonnière, *Inorg. Chem.* **2009**, *48*, 1507–1518; c) P. Kadjane, C. Platas-Iglesias, R. Ziessel, L. Charbonnière, *Dalton Trans.* **2009**, 5688–5700; d) M. Mato-Iglesias, A. Roca-Sabio, Z. Palinkas, D. Esteban-Gomez, C. Platas-Iglesias, E. Toth, A. de Blas, T. Rodriguez-Blas, *Inorg. Chem.* **2008**, *47*, 7840–7851; e) C. Nuñez, R. Bastida, A. Macias, M. Mato-Iglesias, C. Platas-Iglesias, L. Valencia, *Dalton Trans.* **2008**, 3841–3850; f) A. Roca-Sabio, M. Mato-Iglesias, D. Esteban-Gómez, E. Toth, A. de Blas, C. Platas-Iglesias, T. Rodríguez-Blas, *J. Am. Chem. Soc.* **2009**, *131*, 3331–3341.
[25] M. Dolg, H. Stoll, A. Savin, H. Preuss, *Theor. Chim. Acta* **1989**, *75*, 173–194.
[26] a) U. Cosentino, A. Villa, D. Pitea, G. Moro, V. Barone, A. Maiocchi, *J. Am. Chem. Soc.* **2002**, *124*, 4901–4909; b) B. A. Hess Jr., A. Kedziorski, L. Smentek, D. J. Bornhop, *J. Phys. Chem. A* **2008**, *112*, 2397–2407.
[27] a) R. S. Dickins, J. A. K. Howard, C. L. Maupin, J. M. Moloney, D. Parker, J. P. Riehl, G. Siligardi, J. A. G. Williams, *Chem. Eur. J.* **1999**, *5*, 1095–1105; b) S. Zhang, K. Wu, M. C. Biewer, A. D. Sherry, *Inorg. Chem.* **2001**, *40*, 4284–4290; c) S. Amin, D. A. Voss Jr., W. D. Horrocks Jr., C. H. Lake, M. R. Churchill, J. R. Morrow, *Inorg. Chem.* **1995**, *34*, 3294–3300; d) G. Zucchi, R. Scopelliti, J.-C. G. Bünzli, *J. Chem. Soc., Dalton Trans.* **2001**, 1975–1985.
[28] C. Piguet, J.-C. G. Bünzli, G. Bernardinelli, C. G. Bochet, P. Froidevaux, *J. Chem. Soc., Dalton Trans.* **1995**, 83–97.
[29] a) N. Chatterton, Y. Bretonnière, J. Pécaut, M. Mazzanti, *Angew. Chem. Int. Ed.* **2005**, *117*, 7595–7598; b) N. Weibel, L. Charbonnière, R. Ziessel, *Tetrahedron Lett.* **2006**, *47*, 1793–1796.
[30] J.-C. G. Bünzli, in: *Lanthanide Probes in Life, Chemical and Earth Sciences, Theory and Practice* (Eds.: J.-C. G. Bünzli, G. R. Choppin), Elsevier Science Publications, Amsterdam, **1989**, p. 233.
[31] G. Zucchi, A.-C. Ferrand, R. Scopelitti, J.-C. G. Bünzli, *Inorg. Chem.* **2002**, *41*, 2459–2465.
[32] C. Görller-Walrand, K. Binnemans, in: *Handbook on the Physics and Chemistry of Rare Earths* (Eds.: K. A. Gschneider Jr., L. Eyring), Elsevier Science, Amsterdam, **1998**, vol. 25, p. 101.
[33] a) C. Piguet, A. F. Williams, B. Bernardinelli, G. Hopfgartner, S. Petoud, O. Schaad, *J. Am. Chem. Soc.* **1996**, *118*, 6681–6697; b) C. Piguet, E. Rivara-Minten, G. Hopfgartner, J.-C. G. Bünzli, *Helv. Chim. Acta* **1995**, *78*, 1541–1566.
[34] S. T. Frey, W. de Horrocks, *Inorg. Chim. Acta* **1995**, *229*, 383–390.
[35] R. M. Supkowski, W. D. W. Horrocks Jr., *Inorg. Chim. Acta* **2002**, *340*, 44–48.
[36] M. H. V. Werts, R. T. F. Jukes, J. W. Verhoeven, *Phys. Chem. Chem. Phys.* **2002**, *4*, 1542–1548.
[37] P. C. R. Soares-Santos, H. I. S. Nogueira, V. Félix, M. G. B. Drew, R. A. Sá Ferreira, L. D. Carlos, T. Trindade, *Chem. Mater.* **2003**, *15*, 100–108.
[38] M. Latva, H. Takalo, V.-M. Mukkala, C. Matachescu, J. C. Rodriguez-Ubis, J. Kankare, *J. Lumin.* **1997**, *75*, 149–169.
[39] Assuming that the sensitivity of the fluorescence method should allow the observation of spectral changes at a minimum of 5% of a new species, one can estimate a lower limit of 0.1 log units for the association constants of Cl^- and Br^- anions according to Equation (7).
[40] a) R. S. Dickins, D. Parker, J. I. Bruce, D. J. Tozer, *Dalton Trans.* **2003**, 1264–1271; b) B. S. Murray, E. J. New, R. Pal, D. Parker, *Org. Biomol. Chem.* **2008**, *6*, 2085–2094; c) Y. Bretonniere, M. J. Cann, D. Parker, R. Slater, *Org. Biomol. Chem.* **2004**, *2*, 1624–1632.
[41] H. Gampp, M. Maeder, C. J. Meyer, A. D. Zuberbühler, *Talanta* **1985**, *32*, 251–264.
[42] P. L. Jones, A. J. Amoroso, J. C. Jeffery, J. A. McCleverty, E. Psillakis, L. H. Rees, M. D. Ward, *Inorg. Chem.* **1997**, *36*, 10–18.
[43] D. D. Perrin, in: *Ionization Constants of Inorganic Acids and Bases in Aqueous Solution*, 2nd ed., Pergamon, Oxford, **1982**.
[44] Y. Haas, G. Stein, *J. Phys. Chem.* **1971**, *75*, 3668–3677.
[45] K. Nakamaru, *Bull. Chem. Soc. Jpn.* **1982**, *55*, 1639–1640.

 © 2010 Wiley-VCH Verlag GmbH & Co. KGaA, Weinheim

[46] J. Olmstead, *J. Phys. Chem.* **1979**, *83*, 2581–2584.
[47] B. Valeur, in: *Molecular Fluorescence*, Wiley-VCH, Weinheim, Germany, **2002**, p. 161.
[48] a) A. D. Becke, *J. Chem. Phys.* **1993**, *98*, 5648–5652; b) C. Lee, W. Yang, R. G. Parr, *Phys. Rev. B* **1988**, *37*, 785–789.
[49] M. J. Frisch, G. W. Trucks, H. B. Schlegel, G. E. Scuseria, M. A. Robb, J. R. Cheeseman, J. A. Montgomery Jr., T. Vreven, K. N. Kudin, J. C. Burant, J. M. Millam, S. S. Iyengar, J. Tomasi, V. Barone, B. Mennucci, M. Cossi, G. Scalmani, N. Rega, G. A. Petersson, H. Nakatsuji, M. Hada, M. Ehara, K. Toyota, R. Fukuda, J. Hasegawa, M. Ishida, T. Nakajima, Y. Honda, O. Kitao, H. Nakai, M. Klene, X. Li, J. E. Knox, H. P. Hratchian, J. B. Cross, V. Bakken, C. Adamo, J. Jaramillo, R. Gomperts, R. E. Stratmann, O. Yazyev, A. J. Austin, R. Cammi, C. Pomelli, J. W. Ochterski, P. Y. Ayala, K. Morokuma, G. A. Voth, P. Salvador, J. J. Dannenberg, V. G. Zakrzewski, S. Dapprich, A. D. Daniels, M. C. Strain, O. Farkas, D. K. Malick, A. D. Rabuck, K. Raghavachari, J. B. Foresman, J. V. Ortiz, Q. Cui, A. G. Baboul, S. Clifford, J. Cioslowski, B. B. Stefanov, G. Liu, A. Liashenko, P. Piskorz, I. Komaromi, R. L. Martin, D. J. Fox, T. Keith, M. A. Al-Laham, C. Y. Peng, A. Nanayakkara, M. Challacombe, P. M. W. Gill, B. Johnson, W. Chen, M. W. Wong, C. Gonzalez, J. A. Pople, *Gaussian 03*, Revision C.01, Gaussian, Inc., Wallingford, CT, **2004**.
[50] a) L. Maron, O. Eisenstein, *J. Phys. Chem. A* **2000**, *104*, 7140–7143; b) C. Boehme, B. Coupez, G. Wipff, *J. Phys. Chem. A* **2002**, *106*, 6487–6498; c) K. I. M. Ingram, M. J. Tassell, A. J. Gaunt, N. Kaltsoyannis, *Inorg. Chem.* **2008**, *47*, 7824–7833.
[51] V. Vetere, P. Maldivi, C. Adamo, *J. Comput. Chem.* **2003**, *24*, 850–858.
[52] a) G. Gran, *Analyst* **1952**, *77*, 661; b) A. E. Martell, R. J. Motekaitis, in: *Determination and Use of Stability Constants*, 2nd ed., Wiley, New York, **1992**.
[53] P. Gans, A. Sabatini, A. Vacca, *Talanta* **1996**, *43*, 1739–1753.

Received: October 28, 2009
Published Online: January 21, 2010

 © 2010 Wiley-VCH Verlag GmbH & Co. KGaA, Weinheim